ANNALS OF PHYSICS 78, 391–420 (1973)

On the Ground State of an Impurity in a Dilute Fermi Gas*

R. F. BISHOP†

Institute of Theoretical Physics, Department of Physics, Stanford University, Stanford, California 94305

Received June 28, 1972

The system under consideration is a large collection of identical fermions (B), forming a background, into which is inserted a relatively small number of distinct impurity (I) particles. The background is considered to be dilute in the sense that $R \gg a$, where R is the average separation of the B particles, and a is the range of their interaction potential; and the I particles are so dilute with respect to the B particles that I–I interactions can be ignored. The I particles are then all essentially at rest in their ground state. The BB and BI interaction potentials are chosen to be hard cores of the same range a. A series expansion is developed for the ground-state energy of the I particles, and the first four terms are calculated explicitly using two distinct methods, employing Feynman and Goldstone diagrams respectively. It is shown that each method has distinct advantages over the other, and that a judicious combination of both can be used to considerable benefit.

1. INTRODUCTION

A previous paper [1] (hereafter referred to as A) by this author investigated the ground-state properties of a dilute gas of identical fermions interacting in general via a repulsive two-body potential, where in particular this was chosen as the extreme hard-core potential. (The restriction to repulsive potentials was necessary to avoid the complication of the possibility of Cooper pair [2] formation, leading to a superconducting state of lower energy than the normal ground state.) This model problem provides a crude approximation to several systems of physical interest, e.g., nuclear matter; liquid He^3.

In this paper we wish to consider the extension of the model to the case where an impurity particle, or a dilute concentration of impurity particles, is added to the original many-body system. The density of the impurity particles is understood

* Research sponsored by the Air Force Office of Scientific Research, Office of Aerospace Research, U. S. Air Force under AFOSR Contract No. F44620-71-C-0044.

† Present address: Department of Theoretical Physics, University of Manchester, Manchester, England.

to be dilute in the sense that interactions between impurities can be neglected. We can consider such a model as providing a first approximation to such physical systems as (i) a dilute admixture of liquid He^4 in liquid He^3, and (ii) a Λ-particle in nuclear matter, i.e., the extrapolation from finite hypernuclei to the usual limit of nuclear matter.

Two methods for calculating the ground-state energy of the pure many-fermion system were discussed in [*A*], where they were referred to as the *G* and *F* methods respectively. Both methods involve rearrangement of the usual many-body perturbation series in powers of the interaction potential, so that the potential is eliminated in favor of a scattering function which sums the ladder diagrams for multiple scatterings between a pair of particles. The main difference between the methods is then that the *G* method employs time-dependent perturbation theory (Goldstone diagrams), while the *F* method uses a time-independent formalism (Feynman diagrams).

For the pure Fermi gas of hard spheres of diameter a, the dimensionless expansion parameter is $c = k_F a$, where k_F is the Fermi wavenumber. It was shown in [*A*] that the first three terms in the perturbation series for the ground-state energy are proportional to powers of c through cubic order, and that after this point divergent terms enter. Thus the next term in the series is proportional to $c^4 \ln c$. For the pure Fermi gas, these four terms were calculated explicitly in [*A*] for a general repulsive two-body potential, and they were shown to depend only on the low-energy two-body scattering parameters. Beginning with the next term in the series, i.e. with the term proportional to c^4 for the hard-core potential, parameters from three-body scattering were shown to enter. The calculations in [*A*] were performed in detail for the *G* method, and it was shown how the same results are obtained using the *F* method. One of the conclusions of the investigation was that the two methods tend to complement each other.

In this paper we shall use the two methods discussed in [*A*] to derive the ground-state energy of an impurity in a Fermi gas. The complementarity of the two methods is exploited, and the methods are compared in greater detail than in [*A*]. A somewhat surprising outcome of the investigation is that in the case where the impurity and background particles have equal mass, an exact analytic expression can be obtained for each term in the series for the ground-state energy of an impurity particle, examined to the same order as in *A*. This fact greatly facilitates the comparison of the two methods.

The problem of a hard-core impurity in a dilute background of identical fermions was first investigated by Walecka [3] in the context of the infinite hypernucleus problem (see [4] for an excellent review of the hypernuclear problem). He derived an expression for the ground-state energy of a Λ-particle imbedded in nuclear matter to $O(a^2)$, where a is the diameter of the ΛN hard-core interaction, using the Bethe-Goldstone [5] equation for the problem.

These results were verified in a previous paper [6] by this author, using the Green function formulation employing Feynman diagrams. To the knowledge of this author, no other calculations for the "impure system" have been performed, in the case of the hard-core interaction. It is the purpose of the present work to indicate how the two methods can be extended, and in particular to find the next two terms in the series for the ground-state energy, proportional to c^3 and $c^4 \ln c$, respectively.

In Section 2 the two methods are discussed, and the relevant scattering functions are derived. The series for the ground-state energy of the impurity particles is calculated through terms proportional to c^3 in Section 3, using the F method; and in Section 4 the G method is used to derive the same results. In Section 5, the next term in the series expansion is shown to be proportional to $c^4 \ln c$, and its coefficient is calculated. The results are summarized in Section 6, and a comparison of the two methods is presented. Some integrals needed for the calculations are evaluated in the Appendix.

2. The Methods and Notation

The many-fermion background is considered to be comprised of a large number N of identical particles (labeled B) of mass m_B, each having ν spin and isospin degrees of freedom. If the system is confined to a volume Ω, then in the ground-state the momentum distribution fills the Fermi sphere of radius k_F, given by

$$\frac{N}{\Omega} = \nu \frac{k_F^3}{6\pi^2}. \tag{2.1}$$

(Henceforth, we employ a system of units in which $\hbar = \Omega = 1$). Into this background an impurity particle (labeled I) of mass m_I, or a dilute concentration of such impurity particles is inserted. The number density of impurity particles can be related to a corresponding impurity Fermi momentum by a relation equivalent to Eq. (2.1). We are concerned only with the case where the density of impurities, and hence also their Fermi momentum, is vanishingly small. In this case, the impurity particles will be essentially at rest in the lowest state, and interactions between impurity particles can be ignored.

The background particles are considered to interact via a repulsive two-body (BB) potential which, in particular, is chosen to be a hard-core interaction of range a. The impurity particles interact with the background particles via a two-body (BI) potential, which is also chosen to be a hard-core interaction. For ease, both the background and impurity particles are considered as hard spheres of the same diameter a. The only dimensionless parameter characterizing the system is then $c \equiv k_F a$, and the background is considered to be dilute enough so that $c \ll 1$.

It is trivial to extend our results to the case where the background and impurity particles are hard spheres of different sizes, but in applications to problems of physical interest, the case of equal size is probably reasonable. Thus, for the infinite hypernucleus, the real ΛN interaction presumably includes a hard core of about the same radius as in the NN interaction [7].

The two methods of interest to us have been examined in detail in [A] for the case of a pure many-fermion system. In both cases the interparticle potential V is eliminated in favor of the relevant scattering matrix, referred to generically as the $\mathscr{T}$-matrix to cover the three cases of free scattering (t-matrix and k-matrix), and scattering in the presence of the filled Fermi background by both the F method (T-matrix) and the G method (K-matrix). For the case of free scattering (i.e., *in vacuo*) the t-matrix differs from the k-matrix only in the specification of the boundary condition at infinity; the former being defined in terms of the outgoing-wave boundary condition, and the latter in terms of the standing-wave boundary condition. Similarly, the K-matrix describes the scattering of two particles outside the Fermi sea (with a standing-wave boundary condition), whereas the T-matrix describes the scattering of both two particles outside the Fermi sea (with an outgoing-wave boundary condition) and two holes inside the Fermi sea (with an incoming-wave boundary condition). In the present case, both the BB potential (V_{BB}) and the BI potential (V_{BI}) are eliminated in favor of the generic functions $\mathscr{T}_{BB}$ and $\mathscr{T}_{BI}$ respectively.

The results of Section 2 of [A] are easily generalized to the case where the two scattering particles are not identical. The $\mathscr{T}$-matrix that describes the scattering of particles 1 and 2 with initial and final momenta given by p_1, p_2 and p_1', p_2' respectively is defined by the solution to the following integral equation.

$$
\begin{aligned}
&i\mathscr{T}_{1,2}(p_1, p_2; p_1', p_2') \\
&\quad = iu(\mathbf{p}_1, \mathbf{p}_2; \mathbf{p}_1', \mathbf{p}_2') - \frac{1}{2\mu}\int \frac{d^4q}{(2\pi)^4}\, \mathscr{T}_{1,2}(p_1 - q, p_2 + q; p_1', p_2') \\
&\qquad \times \mathscr{G}_1^0(p_1 - q)\, \mathscr{G}_2^0(p_2 + q)\, u(\mathbf{p}_1, \mathbf{p}_2; \mathbf{p}_1 - \mathbf{q}, \mathbf{p}_2 + \mathbf{q}),
\end{aligned} \tag{2.2}
$$

where

$$u = 2\mu V; \qquad \mu = m_1 m_2/(m_1 + m_2).$$

In Eq. (2.2), the function $\mathscr{G}_i^0(p)$ is the relevant single-particle propagator for particle i, and the three cases are distinguished only by the different expressions for this function. Since we are dealing with a translationally invariant system, it is convenient to transform to the c.m. frame, where

$$
\begin{aligned}
&P = p_1 + p_2 = p_1' + p_2', \qquad p = (m_2 p_1 - m_1 p_2)/(m_1 + m_2), \\
&p' = (m_2 p_1' - m_1 p_2')/(m_1 + m_2), \qquad u(\mathbf{p}_1, \mathbf{p}_2; \mathbf{p}_1', \mathbf{p}_2') = u(\mathbf{p} - \mathbf{p}').
\end{aligned}
$$

Transformation of Eq. (2.2) then shows that $\mathscr{T}_{1,2}(\mathbf{p}, \mathbf{p}'; P) = \mathscr{T}_{1,2}(p_1, p_2; p_1', p_2')$ satisfies the integral equation

$$\mathscr{T}_{1,2}(\mathbf{p}, \mathbf{p}'; P) = u(\mathbf{p} - \mathbf{p}') - \int \frac{d^3q}{(2\pi)^3} u(\mathbf{p} - \mathbf{q})\, g_{1,2}(\mathbf{q}, P)\, \mathscr{T}_{1,2}(\mathbf{q}, \mathbf{p}'; P), \quad (2.3)$$

where

$$g_{1,2}(\mathbf{q}, P) = -\frac{i}{2\mu} \int \frac{dq_0}{2\pi}\, \mathscr{G}_1^0\left(\frac{\mu}{m_2} P + q\right) \mathscr{G}_2^0\left(\frac{\mu}{m_1} P - q\right). \quad (2.4)$$

These relations can now be specialized to the three cases of interest to us, for both $\mathscr{T}_{BB}$ and $\mathscr{T}_{BI}$, exactly as in (A). Thus, for the F method, Eq. (2.3) becomes (the ladder approximation to) the Bethe–Salpeter equation [8], and similarly for the G method, Eq. (2.3) represents the Bethe–Goldstone equation [5]. The relation between these two equations for the present problem has been investigated in some detail in [6]. The three forms for $\mathscr{G}_B^0$ that distinguish the three cases are given in Section 2 of (*A*), and those for $\mathscr{G}_I^0$ are identical except that the Fermi momentum for the impurity particles (I) is allowed to go to zero. In the F method, Eq. (2.3) is now specialized to the equation for the T-matrix, and the potential u is eliminated between this equation and a similar equation for the free scattering t-matrix, which is known exactly for the hard-core potential [9]. Thus, if Eq. (2.3) is written in operator notation as

$$\mathscr{T}(P) = u - ug(P)\,\mathscr{T}(P),$$

we find, by specializing to the two cases of interest to us, that

$$T(P) = u - ug^F(P)\, T(P), \quad (2.5)$$

and

$$t(s) = u - ug^0(s)\, t(s) = u - t(s)\, g^0(s) u. \quad (2.6)$$

The potential u may be eliminated between Eq. (2.5) and the second of Eqs. (2.6) to give

$$\begin{aligned} T(P) &= t(s) + t(s)\, \Delta g(P)\, T(P), \\ \Delta g(P) &= g^0(s) - g^F(P). \end{aligned} \quad (2.7)$$

By iterating Eq. (2.7), the T-matrix can be obtained to any desired order in a. The final result follows exactly as in (*A*), and the following expressions are readily verified.

$$T_{1,2}(\mathbf{p}, \mathbf{p}'; P) = 4\pi a + \frac{2\pi}{3} a^3(4s - p^2 - p'^2 + 6\mathbf{p} \cdot \mathbf{p}') + (4\pi a)^2 J_{1,2}(P) + (4\pi a)^3 J_{1,2}^2(P) + O(a^4), \tag{2.8a}$$

$$J_{1,2}(P) = \int \frac{d\mathbf{q}}{(2\pi)^3} \Delta g_{1,2}(\mathbf{q}, P) - \frac{i\kappa}{4\pi},$$

where

$$\Delta g_{BB}(\mathbf{q}, P) = (q^2 - s - i\eta)^{-1} - N(\mathbf{q}, \mathbf{P})[q^2 - s - i\eta N(\mathbf{q}, \mathbf{P})]^{-1},$$
$$N(\mathbf{q}, \mathbf{P}) = 1 - n(\tfrac{1}{2}\mathbf{P} + \mathbf{q}) - n(\tfrac{1}{2}\mathbf{P} - \mathbf{q}); \tag{2.8b}$$

and

$$\Delta g_{BI}(\mathbf{q}, P) = n((\mu/m_I)\mathbf{P} + \mathbf{q})(q^2 - s - i\eta)^{-1}, \tag{2.8c}$$

where η is a positive infinitesimal. In the above expressions, the quantity $s/(2\mu)$ is just the total c.m. energy of the scattering pair,

$$s = 2\mu\{P_0 - \mathbf{P}^2/2(m_1 + m_2)\}, \qquad \kappa = +s^{1/2}, \tag{2.9}$$

and $n(k)$ is the Fermi momentum distribution function of the background particles,

$$n(k) = \theta(k_F - |\,\mathbf{k}\,|),$$

where $\theta(x)$ is the usual unit-step function, equal to one for $x > 0$ and zero for $x < 0$.

The K-matrix of the G method is obtained similarly as

$$K_{1,2}(\mathbf{p}, \mathbf{p}'; P) = 4\pi a + \frac{2\pi}{3} a^3(4s - p^2 - p'^2 + 6\mathbf{p} \cdot \mathbf{p}') + (4\pi a)^2 I_{1,2}(P) + (4\pi a)^3 I_{1,2}^2(P) + O(a^4), \tag{2.10a}$$

$$I_{1,2}(P) = \int \frac{d\mathbf{q}}{(2\pi)^3} \Delta \bar{g}_{1,2}(\mathbf{q}, P),$$

where

$$\Delta \bar{g}_{BB}(\mathbf{q}, P) = [1 - \{1 - n(\tfrac{1}{2}\mathbf{P} + \mathbf{q})\}\{1 - n(\tfrac{1}{2}\mathbf{P} + \mathbf{q})\}](q^2 - s)^{-1}, \tag{2.10b}$$

and

$$\Delta \bar{g}_{BI}(\mathbf{q}, P) = n((\mu/m_I)\mathbf{P} + \mathbf{q})(q^2 - s)^{-1}. \tag{2.10c}$$

The energy denominators in the integral for $I_{1,2}(P)$ contain no imaginary infinitesimal term $(i\eta)$ in keeping with the standing-wave boundary condition for the K-matrix, and the integrals are to be understood as principal value integrals.

The expressions for the T- and K-matrices given in Eqs. (2.8–2.10) now form the starting point for the calculations of the ground-state energy of the impurity particles, by the F and G methods respectively. Both methods use diagramatic perturbation series, originally formulated in powers of the interaction potential. Thus the F method employs the diagramatic series for the proper self-energy $\Sigma(p)$ for the impurity particle, while the G method uses the linked-cluster perturbation series of Goldstone [10]. The ground-state energy E_I of the impurities is given directly by the difference in the linked-cluster series for the entire system (background plus impurities), minus the series for the background particles alone.

In each case the diagrams containing the potential operators are regrouped in such a way that the potential can be eliminated in favor of the relevant $\mathcal{T}$-matrix, so that each potential diagram is counted once and once only. For the case of a pure system, the rules for achieving this were described in [A]. In the present case the rules are identical, with some added restrictions described in Sections 3 and 4, due to the assumed dilution of the impurities. Essentially, this restricts the diagrams in each case to those containing the minimal number of impurity hole lines, viz. one in the G case (since the G diagrams are fully contracted), and zero in the F case. In both methods we work in the thermodynamic limit (number of background particles, $N \to \infty$) from the outset. The procedures are described more fully in Sections 3 and 4 where the ground-state energy of the impurity particles is calculated to $O(a^3)$, by the F and G methods respectively.

3. Ground-State Energy of Impurities (F Method)

The full Green function propagator for the impurity particles is defined as

$$G_I(x - x') = -i\langle A \mid T\{\psi_I(x)\, \psi_I^{\dagger}(x')\} \mid A\rangle,$$

where $\psi_I(x)$ is the Heisenberg operator for the I-field, $\mid A\rangle$ is the exact many-body Heisenberg ground state of the background particles, and T is the usual time-ordering operator. For a very dilute concentration of impurity particles (i.e., when I–I interactions can be ignored), the function G_I defined above propagates only forward in time. Written in the momentum–space representation in terms of the usual proper self-energy operator for the I-particles, $\Sigma(p_\mu) \equiv \Sigma(\mathbf{p}, p_0)$, G_I takes the form

$$G_I(p_\mu) = [p_0 - (\mathbf{p}^2/2m_I) - \Sigma(p_\mu)]^{-1}.$$

The single-particle excitation spectrum $\epsilon_I(p)$ for the impurities is given by the poles of the full propagator $G_I(p_\mu)$, that is by the solution for p_0 to the equation

$$p_0 = (\mathbf{p}^2/2m_I) + \Sigma(\mathbf{p}, p_0). \tag{3.1}$$

The ground-state energy per particle is thus given by $\epsilon_I(0) \equiv \epsilon$. If we represent the expansion in powers of the hard-core radius a, of $\Sigma(p_\mu)$ by

$$\Sigma(p_\mu) = \sum_n a^n \Sigma^{(n)}(p_\mu),$$

then Eq. (3.1) can be solved iteratively to yield

$$\begin{gathered}\epsilon = a\Sigma^{(1)} + a^2\Sigma^{(2)}(0) + a^3\left\{\Sigma^{(3)}(0) + \Sigma^{(1)}\frac{d\Sigma^{(2)}(0)}{dp_0}\right\} + \cdots \\ \Sigma^{(n)}(p_0) \equiv \Sigma^{(n)}(0, p_0).\end{gathered} \tag{3.2}$$

In solving Eq. (3.1), we have used the fact that $\Sigma^{(1)}(p_0) = \Sigma^{(1)}$, a constant term, independent of p_0 as we shall see below.

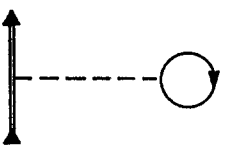

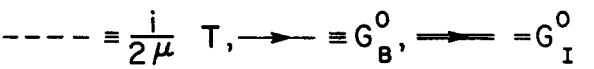

FIG. 1. The only first-order diagram for $\Sigma(p_\mu)$.

In the first place, we shall be interested in computing ϵ to $O(a^3)$, and we must therefore consider all diagrams for $\Sigma(p_\mu)$ containing three or fewer T-matrices. The only first-order diagram is shown in Fig. 1, where the order of a diagram is the total number of T-matrix interactions that it contains. The contribution of this diagram to $\Sigma(p)$ is given by the expression

$$-\frac{i}{2\mu}\int \frac{d^4k}{(2\pi)^4}\, G_B^0(k)\, \nu T_{BI}(p, k; p, k), \tag{3.3}$$

where ν is the number of spin and isospin degrees of freedom of each background particle, and $G_B^0(k)$ is the free (Feynman) propagator for the background particles,

$$G_B^0(k) = [k_0 - (\mathbf{k}^2/2m_B) + i\eta\ \mathrm{sgn}(k - k_F)]^{-1}\, e^{ik_0\eta}, \tag{3.4}$$

where η is a positive infinitesimal. Substituting into Eq. (3.3) for T_{BI} from Eqs. (2.8a, c), leads to the contribution to ϵ from the diagram of Fig. 1. Correct to $O(a^3)$, the expression of Eq. (2.8a) for the function T_{BI} contains three terms; the first purely algebraic, and the second and third proportional to $J_{BI}(P)$ and $J_{BI}^2(P)$ respectively. We denote the contributions to ϵ of these three terms by ϵ_1, ϵ_2, and ϵ_3 respectively.

By direct substitution into Eq. (3.3) the contribution ϵ_1 is trivially found to be

$$\begin{aligned} \epsilon_1 &= (k_F^2/2\mu)\, \nu[(2/3\pi)\, c + (2/15\pi)(1+\alpha)^2\, c^3], \\ c &\equiv k_F a; \qquad \alpha \equiv (m_I - m_B)/(m_I + m_B). \end{aligned} \tag{3.5}$$

It is also apparent that $\Sigma^{(1)}(k_0)$ is independent of k_0, as needed in the derivation of Eq. (3.2).

The contribution ϵ_2 is similarly shown to be given by the expression

$$\epsilon_2 = (4\pi a)^2 \frac{\nu}{2\mu} \int \frac{d\mathbf{k}}{(2\pi)^3}\, n(k) \int \frac{d\mathbf{q}}{(2\pi)^3} \frac{n(q)}{q^2 - (1-\alpha)\,\mathbf{k}\cdot\mathbf{q} - \alpha k^2}.$$

The integrations are elementary, and the final result below is easily obtained.

$$\epsilon_2 = \left(\frac{k_F^2}{2\mu}\right) \nu \frac{(1-\alpha)}{4\pi^2\alpha^2} \left[(1+\alpha)^2 \ln\frac{1+\alpha}{1-\alpha} - 2\alpha\right] c^2. \tag{3.6}$$

The contribution ϵ_3 is found in the same way to be given by the expression

$$\epsilon_3 = (4\pi a)^3 \frac{\nu}{2\mu} \int \frac{d\mathbf{k}}{(2\pi)^3}\, n(k) \left\{\int \frac{d\mathbf{q}}{(2\pi)^3} \frac{n(q)}{q^2 - (1-\alpha)\,\mathbf{k}\cdot\mathbf{q} - \alpha k^2}\right\}^2,$$

which is readily reduced to the one-dimensional integration of

$$\begin{aligned} \epsilon_3 &= \left(\frac{k_F^2}{2\mu}\right) \nu \left(\frac{2}{\pi^3}\right) \frac{c^3}{(1-\alpha)^2} \int_0^1 dx\, [f(x) - f(\alpha x)]^2, \\ f(x) &\equiv \frac{1}{2}(1-x^2) \ln\left|\frac{1+x}{1-x}\right| + x. \end{aligned} \tag{3.7}$$

In the general case of unequal masses for the impurity and background particles ($\alpha \neq 0$), the remaining integral must be performed numerically. For equal masses however, the integral is performed analytically in the appendix. We give the results for both the equal mass case, and for the infinite hypernucleus problem (i.e., B = nucleon ($\nu = 4$), mass $m_N = 939$ MeV: $I = \Lambda$-particle, mass $m_\Lambda = 1115$ MeV).

$$\epsilon_3 = \begin{cases} \left(\frac{k_F^2}{m}\right) \nu \frac{2}{\pi^3} \left(\frac{2\pi^2}{45} + \frac{1}{3}\right) c^3; & m_B = m_I \equiv m, \\ \left(\frac{k_F^2}{2\mu}\right) (0.189)\, c^3; & B \equiv N, \quad I \equiv \Lambda. \end{cases} \tag{3.8}$$

The expressions ϵ_1, ϵ_2, and ϵ_3 exhaust the contribution to the ground-state energy per impurity from the first-order diagram, to $O(c^3)$. There is actually one further term that arises from the first-order diagram, due to the last factor $[a^3 \Sigma^{(1)} \Sigma^{(2)\prime}(0)]$ in Eq. (3.2), but we show below that this contribution to ϵ is exactly cancelled by the leading contribution from a third-order diagram.

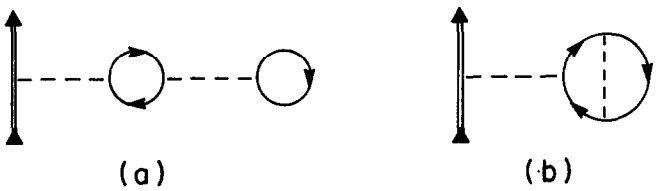

FIG. 2. The two second-order T-matrix diagrams for $\Sigma(p_\mu)$.

We now turn to the second-order T-matrix diagrams, of which there are two, as shown in Fig. 2. The contribution of these two diagrams to $\Sigma(0)$ is readily shown to be given by the expression

$$\Sigma_2(0) = -\frac{\nu}{(2\mu)^2} \int \frac{d^4k}{(2\pi)^4} \int \frac{d^4l}{(2\pi)^4} \{G_B^0(k)\}^2\, G_B^0(l)\, T_{BI}(0, k; 0, k) \times [\nu T_{BB}(k, l; k, l) - T_{BB}(k, l; l, k)].$$

By substituting from Eq. (2.8) for the T-matrices, this expression can be evaluated to $O(a^3)$. The iterations to this order can be represented pictorially as in Fig. 3, where the dotted line represents the T-matrix interaction to lowest order, and a crosshatched pair of lines represents the restricted two particle propagator, given in Eq. (2.8) in the c.m. representation. In Fig. 3, the diagrams (a.i)–(a.iii) and (b.i)–(b.iii) thus represent the evaluation of diagrams (a) and (b) respectively of Fig. 2 to $O(a^3)$. By direct evaluation, it can be easily seen that diagrams (a.i) and (b.i) of Fig. 3 give an identically zero contribution to $\Sigma(p)$. This comes about because in both cases a particle and a hole are required to be in the same momentum state. Thus, the contribution ϵ_2 of Eq. (3.6) exhausts the $O(c^2)$ contribution to the ground-state energy. For the infinite hypernucleus problem this contribution was first evaluated by Walecka [3], who used the G method, and was verified in a previous paper by this author [6], using the F method. Continuing with the evaluation of the second-order T-matrix diagrams, by direct computation it is easy to

show that both diagrams (a.iii) and (b.iii) give vanishing contribution to ϵ. Similarly it is not difficult to show that the remaining diagrams, (a.ii) and (b.ii), of Fig. 3 exactly cancel the $O(a^3)$ contribution from the two third-order T-matrix diagrams of Fig. 4.

Thus, the diagrams of Figs. 2 and 4 taken together give an identically zero contribution, to $O(a^3)$, to the proper self-energy operator $\Sigma(p_\mu)$. Similar cancel-

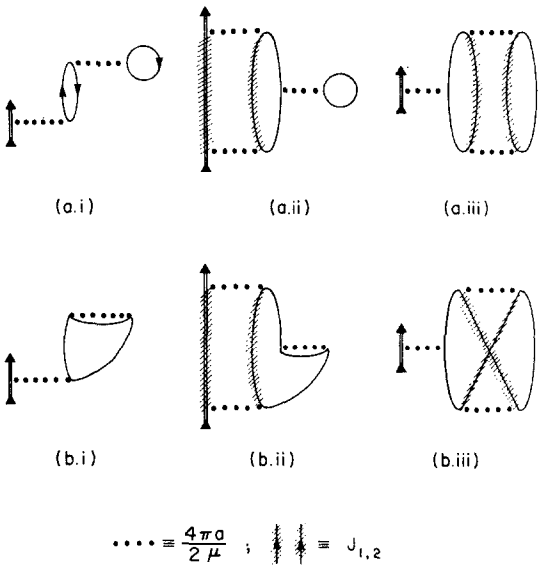

FIG. 3. The diagrams of Fig. 2 iterated to $O(a^3)$.

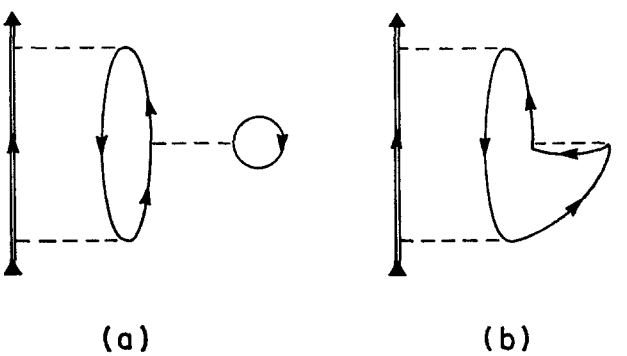

FIG. 4. To lowest order $[O(a^3)]$, diagrams (a) and (b) exactly cancel against diagrams (a.ii) and (b.ii) of Fig. 3, respectively.

lations and vanishing contributions also occur in higher orders. We shall see in the next section that much of this cumbersome "bookkeeping" is taken care of automatically in the G method, and thus gives it an advantage over the F method.

Having completed the discussion of the diagrams containing two T-matrices, the evaluation of ϵ to $O(a^3)$ can be concluded by enumerating the remaining third-order diagrams. These diagrams can conveniently be divided into classes distinguished by the number of BI interactions. It is trivial to show by direct evaluation that to $O(a^3)$, all of the diagrams containing just one T_{BI}-matrix, examples of which are shown in Fig. 5, are identically zero.

There are two third-order diagrams containing three T_{BI}-matrix interactions, shown in Fig. 6. Let us denote the contributions to ϵ to $O(a^3)$ of the two diagrams of Fig. 6(a), (b) by ϵ' and ϵ_4 respectively. By direct evaluation of the first diagram we find

$$\epsilon' = (-\nu)^2 i^3 \left(\frac{4\pi a}{2\mu}\right)^3 \int \frac{d^4t\, d^4k\, d^4l}{(2\pi)^{12}} G_B^0(t)\, G_B^0(k)\, G_B^0(l)\{G_I^0(k-t)\}^2,$$

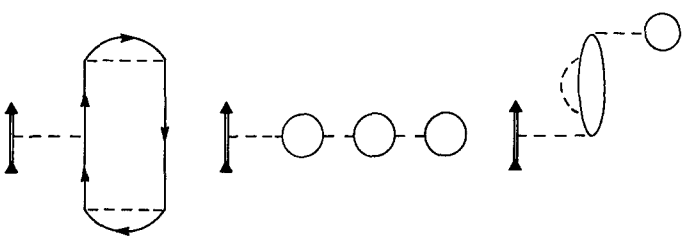

FIG. 5. Diagrams for $\Sigma(p_\mu)$ containing one T_{BI} interaction and two T_{BB} interactions.

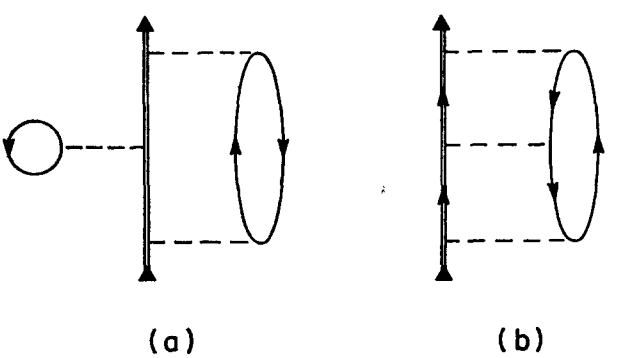

FIG. 6. The two third-order diagrams for $\Sigma(p_\mu)$ containing three T_{BI}-matrix interactions.

and by inserting the explicit forms for the propagators, hence

$$\epsilon' = \nu^2 \left(\frac{4\pi a}{2\mu}\right)^3 \frac{1}{(2\pi)^9} \left(\frac{4\pi k_F^3}{3}\right) \int d\mathbf{t}\, d\mathbf{k}\, n_k(1 - n_t) \Big/ \left[\frac{t^2 - k^2}{2m_B} - \frac{|\mathbf{t} - \mathbf{k}|^2}{2m_I}\right]^2. \tag{3.9}$$

We shall now show that this term is exactly cancelled by the last term in Eq. (3.2), namely

$$\epsilon'' = a^3 \Sigma^{(1)}\, d\Sigma^{(2)}(0)/dp_0\,. \tag{3.10}$$

From our discussion above it is clear that the only contributions to $\Sigma^{(1)}$ and $\Sigma^{(2)}(p_0)$ come from the first-order diagrams of Fig. 1, and by direct evaluation from Eq. (3.3) we find

$$\Sigma^{(1)} = \nu(k_F^2/2\mu)(2k_F/3\pi),$$

$$\Sigma^{(2)}(p_0) = \nu \left(\frac{16\pi^2}{2\mu}\right) \int \frac{d\mathbf{k}\, d\mathbf{k}'}{(2\pi)^6} n_k \left[\frac{1}{k'^2 - q^2} + \frac{1 - n((\mu/m_I)\,\mathbf{k} + \mathbf{k}')}{2\mu p_0 + q^2 - k'^2 + i\eta}\right],$$

where

$$\mathbf{q} = (\mu/m_B)\mathbf{k}.$$

From Eq. (3.10) we then find,

$$\epsilon'' = -\nu^2 \left(\frac{4\pi a}{2\mu}\right)^3 \frac{1}{(2\pi)^9} \left(\frac{4\pi k_F^3}{3}\right) \int d\mathbf{k}\, d\mathbf{k}'\, n_k \frac{1 - n((\mu/m_I)\,\mathbf{k} + \mathbf{k}')}{[(q^2 - k'^2)/2\mu]^2}\,.$$

After the substitution $\mathbf{k}' = \mathbf{t} - (\mu/m_I)\mathbf{k}$, this last expression, by comparison with Eq. (3.9), is seen to be given by

$$\epsilon'' = -\epsilon'.$$

Thus the contribution to ϵ of diagram (a) of Fig. 3 is exactly cancelled to $O(a^3)$ by the last term of Eq. (3.2). This cancellation, analogous to a Ward identity, is an example of a whole class of similar cancellations that occur in each order in the F method.

The only other third-order diagram containing three T_{BI}-matrix interactions is that shown in Fig. 6(b), and its contribution to ϵ is thus,

$$\epsilon_4 = (-\nu)\, i^3 \left(\frac{4\pi a}{2\mu}\right)^3 \int \frac{d^4q\, d^4t\, d^4k}{(2\pi)^{12}} G_B^0(q)\, G_B^0(k)\, G_B^0(t)\, G_I^0(k - q)\, G_I^0(t - q),$$

which is easily reduced to the form

$$\epsilon_4 = -\nu \left(\frac{4\pi a}{2\mu}\right)^3 \int \frac{d\mathbf{q}}{(2\pi)^3}(1 - n_q)\left\{\int \frac{d\mathbf{k}}{(2\pi)^3} n_k \Big/ \left[\frac{q^2 - k^2}{2m_B} + \frac{|\mathbf{k} - \mathbf{q}|^2}{2m_I}\right]\right\}^2 \tag{3.11}$$

The **k**-integration is elementary, and expressing the remaining integral in dimensionless form gives the result,

$$\epsilon_4 = -\left(\frac{k_F^2}{2\mu}\right)\nu\left(\frac{2}{\pi^3}\right)\frac{c^3}{(1-\alpha)^2}\int_1^\infty dx\left[f(x) - f\left(\frac{x}{\alpha}\right)\right]^2, \tag{3.12}$$

where $f(x)$ is the same function as defined in Eq. (3.7). When the background and impurity particles have unequal mass ($\alpha \neq 0$), the remaining integral must be performed numerically. For equal mass ($\alpha = 0$) however, the integral can be performed analytically, since

$$f\left(\frac{x}{\alpha}\right) \xrightarrow[\alpha \to 0]{} 0,$$

and the result is given in the appendix as Eq. (A.9). Quoting the results for the same cases as in Eq. (3.8), we find

$$\epsilon_4 = \begin{cases} -\left(\dfrac{k_F^2}{m}\right)\nu\dfrac{2}{\pi^3}\left(\dfrac{4\pi^2}{45} - \dfrac{1}{3}\right)c^3; & m_B = m_I \equiv m, \\ -\left(\dfrac{k_F^2}{2\mu}\right)(0.143)\,c^3; & B \equiv N, \quad I \equiv \Lambda. \end{cases} \tag{3.13}$$

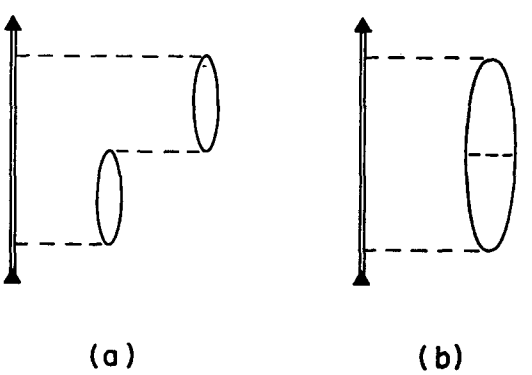

FIG. 7. The two third-order diagrams for $\Sigma(p_\mu)$, containing two T_{BI}-matrix interactions, that contribute to ϵ_5.

The only remaining third-order diagrams are those shown in Fig. 7, containing two T_{BI}-matrix interactions. Apart from the spin and isospin factors, the two diagrams contribute equally to ϵ to $O(a^3)$, and we denote the sum of their contributions by ϵ_5. By direct evaluation of the diagrams, we find

$$\epsilon_5 = \nu(\nu - 1)\, i^3 \frac{(4\pi a)^3}{m_B(2\mu)^2} \int \frac{d^4q}{(2\pi)^4} G_I^0(q) \left\{ \int \frac{d^4t}{(2\pi)^4} G_B^0(t)\, G_B^0(t+q) \right\}^2.$$

It is only possible to evaluate the integrals analytically in the case $m_B = m_I \equiv m$; otherwise they must be performed numerically. In the case of equal mass, the above expression can be written as

$$\epsilon_5 = \nu(\nu - 1)\,(4\pi a/m)^3\, M, \tag{3.14}$$

where M is defined in the appendix in Eqs. (A.10–11), and the result is given in Eq. (A.21). The integration was also performed numerically with the parameters appropriate to the infinite hypernucleus. Thus, the final results are found to be

$$\epsilon_5 = \begin{cases} \left(\frac{k_F^2}{m}\right) \nu(\nu - 1) \frac{8}{3\pi^3} \left(\frac{\pi^2}{8} + \frac{2}{15} \ln 2 - \frac{7}{30}\right) c^3; & m_B = m_I \equiv m, \\ \left(\frac{k_F^2}{2\mu}\right) (1.163)\, c^3; & B \equiv N, \quad I \equiv \Lambda. \end{cases} \tag{3.15}$$

The sum of the expressions ϵ_1 to ϵ_5 thus exhausts the calculation of ϵ to $O(c^3)$. We defer discussion of the next term in the series for ϵ until we have shown how the G method can be used to replicate the above results, which is the subject of Section 4.

4. Ground-State Energy of Impurities (G Method)

In this section we show how the G method can be used to achieve the same results obtained in Section 3 by the F method. The G method uses time-ordered diagrams, and the rules for enumerating the allowed diagrams were given in [*A*] for the pure many-fermion system. In the present case, the rules are the same except that only those diagrams are allowed which contain just one independent[1] impurity hole line. Since the G method uses the completely contracted diagrams corresponding to the Goldstone linked-cluster perturbation series [10], every diagram must include at least one impurity hole line. Since the impurity particles are assumed to be very dilute with respect to the background particles, so that II interactions can be neglected, each independent impurity hole line represents an integration over the vanishingly small Fermi sphere for the I-particles. Thus, a

[1] A number n of propagating lines in a diagram are considered independent if they can be labeled with n independent momentum variables.

G diagram containing n independent impurity hole lines will give a contribution to the total ground-state energy E_I of the N_I impurity particles, proportional to $(N_I)^n$, or equivalently, a contribution to $\epsilon \equiv E_I/N_I$ proportional to $(N_I)^{n-1}$. Consequently only the case $n = 1$ need be considered, as the diagrams for which $n > 1$ will give vanishingly small contribution to ϵ by comparison. In evaluating the diagrams for E_I with $n = 1$, the momentum of the impurity hole can thus be set equal to zero in the energy denominators, and the integration over the hole momentum just gives a factor N_I. The diagrams are otherwise evaluated by the standard rules (given in [*A*]). In drawing the diagrams, the convention is employed that interaction lines are drawn horizontally, and particle (hole) lines are drawn vertically and labeled with an arrow directed up (down).

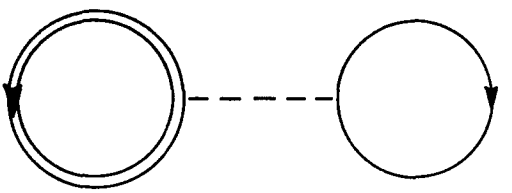

FIG. 8. The only first-order K-matrix diagram for E_I.

To evaluate ϵ to $O(a^3)$ by the G method, we must now consider all the allowed diagrams containing up to three K-matrix interactions. The only diagram containing one K-matrix interaction is shown in Fig. 8, and the contribution, $\epsilon^{(1)}$, of this diagram to ϵ is thus given by the expression

$$\begin{aligned} \epsilon^{(1)} &= \frac{\nu}{2\mu} \int \frac{d\mathbf{p}}{(2\pi)^3}\, n(p)\, K_{BI}(0, \mathbf{p}; 0, \mathbf{p}) \\ &= \frac{\nu}{2\mu} \int \frac{d\mathbf{p}}{(2\pi)^3}\, n(p)\, K_{BI}(\mathbf{k}, \mathbf{k}; k^2); \qquad \mathbf{k} = \tfrac{1}{2}(1 + \alpha)\, \mathbf{p}, \end{aligned} \tag{4.1}$$

where in the second equation the K-matrix has been rewritten in the c.m. representation. This expression can now be evaluated, using the explicit representation of the K-matrix given in Eqs. (2.10a, c). It is trivial to show from Eq. (4.1) that to $O(a^3)$, $\epsilon^{(1)}$ gives just the sum of the terms ϵ_1, ϵ_2, and ϵ_3 of Section 3.

It is now important to realize that, just as dicussed in [*A*], in the G method there are no contributing diagrams containing two K-matrix interactions. The only valid diagrams are those shown in Fig. 9, and in each case, a particle and hole are required to be in the same momentum state, for which there is clearly zero probability. These are the so-called anomalous diagrams, and they may therefore be omitted. By comparison, the F method contains nonzero diagrams containing two T-matrix interactions, although we showed in Section 3, that they contained

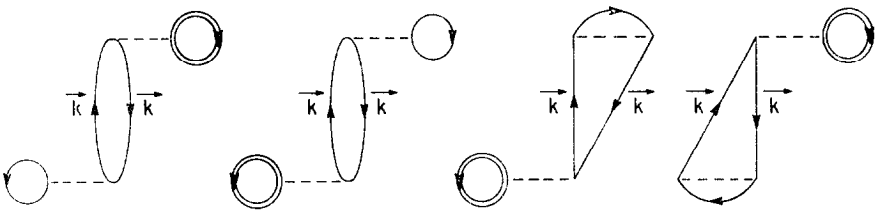

FIG. 9. The only allowed diagrams for E_I containing two K-matrix interactions.

both vanishing pieces and other nonzero terms which were exactly cancelled by higher-order terms. In the G method, what comprised a rather cumbersome amount of "bookkeeping" in the F method, is taken care of trivially. In higher order calculations, this advantage of the G method over the F method can be even more pronounced. By way of contrast however, we shall see below that the F method has its own advantages.

To complete the calculation of ϵ to $O(a^3)$, we therefore have only to consider the diagrams containing three K-matrix interactions. The first set of third-order diagrams that we consider are those containing a first-order self-energy insertion on either a particle or a hole line. Figure 10 shows all the nonanomalous diagrams containing a self-energy insertion on a hole line; this set is labeled H_3. There is a similar set (P_3), obtained by reversing the direction of the arrows shown in Fig. 10, which contain the insertion on a particle line. It is important to realize that diagram (a) of Fig. 10 is valid, because although it contains *two* impurity hole lines, they are

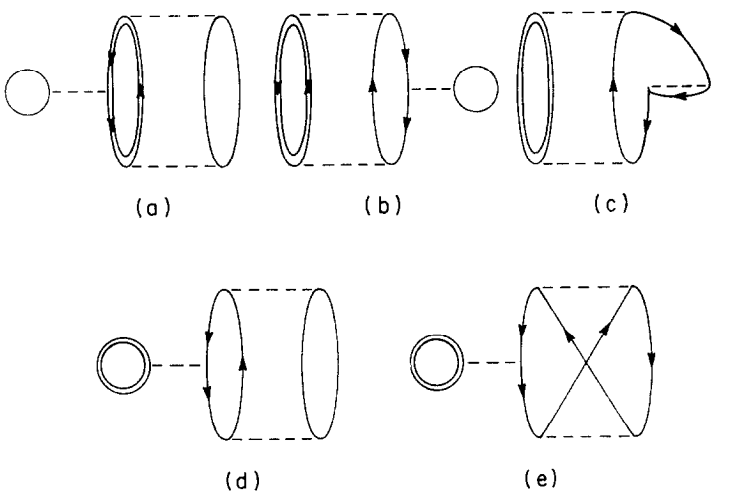

FIG. 10. The set of Goldstone diagrams (H_3) for E_I containing three K-matrix interactions, and having a self-energy insertion on a hole line.

not independent (i.e., both holes are in the same momentum state, and there is thus only one integration over the Fermi sea of the I particles). It is easy to see that to lowest order (i.e., when each K-matrix is replaced by the constant $4\pi a$) each diagram of the set H_3 exactly cancels against the corresponding diagram of P_3, and hence their total contribution to ϵ to $O(a^3)$ is zero. However, this cancellation does not persist to higher orders, as will become apparent when we dicsuss the next (logarithmic) term in the series for ϵ.

The remaining third-order diagrams for E_I contain either two or three K_{BI}-matrix interactions. The only diagram containing three BI interactions is shown in Fig. 11, and it is easy to show that the contribution to ϵ to $O(a^3)$ of this diagram

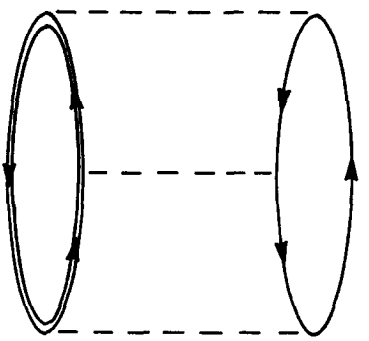

FIG. 11. The only K-matrix diagram that contributes to ϵ_4'.

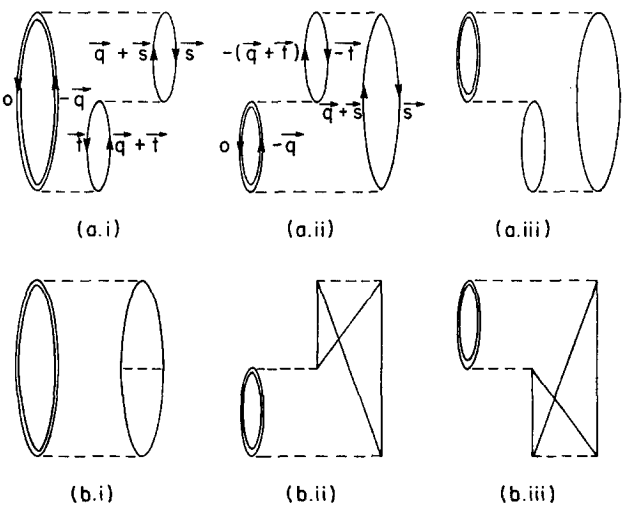

FIG. 12. The six K-matrix diagrams contributing to ϵ_5'.

(ϵ_4', say) is identical with ϵ_4 of Section 3. Thus, evaluating Fig. 11 by the standard rules, we find

$$\epsilon_4' = \left(\frac{4\pi a}{2\mu}\right)^3 \frac{\nu}{(2\pi)^9} (-1)^3 \int d\mathbf{k}\,(1 - n_k) \times \left\{\int d\mathbf{p}\, d\mathbf{q}\, n_q\, \delta(\mathbf{p} + \mathbf{k} - \mathbf{q}) \Big/ \left[\frac{p^2}{2m_I} + \frac{k^2 - q^2}{2m_B}\right]\right\}^2,$$

which is readily identified with ϵ_4 by comparison with Eq. (3.11).

The sole remaining third-order diagrams for E_I are the six diagrams of Fig. 12 containing two *BI* interactions. We denote the total contribution to ϵ of these six diagrams, when evaluated in lowest order, as ϵ_5'. To lowest order, it is easy to see that diagrams (a.i) and (b.i) of Fig. 12 contribute identical amounts to ϵ_5', apart from the trivial difference of spin–isospin factors; and similarly for the remaining four diagrams. If the diagrams (a.i) and (a.ii) are labeled as shown in Fig. 12, and the remaining diagrams are labeled similarly in an obvious way, we find

$$\epsilon_5' = \frac{\nu(\nu - 1)}{(2\pi)^9} \frac{(4\pi a)^3}{(2\mu)^2 m_B} \int d\mathbf{q}\, d\mathbf{s}\, dt\, n_s(1 - n_{\mathbf{q}+\mathbf{s}})\, n_t(1 - n_{\mathbf{q}+\mathbf{t}}) \Big/ \left(\frac{q^2}{2m_I} + \omega_{\mathbf{qs}}\right) \times \left[\left(1 \Big/ \left(\frac{q^2}{2m_I} + \omega_{\mathbf{qt}}\right)\right) + 2/(\omega_{\mathbf{qs}} + \omega_{\mathbf{qt}})\right],$$

where

$$\omega_{\mathbf{qs}} = (1/2m_B)(|\,\mathbf{q} + \mathbf{s}\,|^2 - s^2).$$

It is easy to show that the above expression can be put into the form of Eq. (4.2) which is symmetric between **s** and **t**.

$$\epsilon_5' = \frac{\nu(\nu - 1)}{(2\pi)^9} \frac{(4\pi a)^3}{(2\mu)^2 m_B} \int d\mathbf{q}\, d\mathbf{s}\, dt\, n_s(1 - n_{\mathbf{q}+\mathbf{s}})\, n_t(1 - n_{\mathbf{q}+\mathbf{t}}) \times 2(\omega_{\mathbf{qs}} + \omega_{\mathbf{qt}} + q^2/2m_I)/(\omega_{\mathbf{qs}} + q^2/2m_I)(\omega_{\mathbf{qt}} + q^2/2m_I)(\omega_{\mathbf{qs}} + \omega_{\mathbf{qt}}). \quad (4.2)$$

It is now simple to show that $\epsilon_5' \equiv \epsilon_5$, by direct evaluation of the two *F* diagrams of Fig. 7 which contribute to ϵ_5. However, the actual evaluation of ϵ_5 is much more easily accomplished (either exactly or numerically) by the method used in the appendix, rather than by direct evaluation of Eq. (4.2). The method used in the appendix hinges on the four-momentum formalism of the *F* method, as opposed to the three-momentum formalism of the *G* method. We see that the *F* method in this case is considerably simpler than the *G* method, since it not only combines a large number of *G* diagrams (six in this case) into a smaller number of *F* diagrams

(two in this case), but also provides a simpler method for their evaluation. Similar situations occur in higher orders, where the difference between the two methods can be even more pronounced, and such cases provide one of the main advantages of the F method over the G method.

Having now shown that to $O(a^3)$ the two methods agree (as of course they must), we turn to an investigation of the next term in the series for ϵ, continuing with the G method.

5. Logarithmic Term in Series Expansion of ϵ

In the last two sections we saw that the first three terms in the series for the ground-state energy of the impurity particles were respectively proportional to the first three integral powers of the parameter c. One would therefore expect that the next term in the series should be proportional to c^4. It is not difficult to see that this is not the case however. The root of the problem rests with the expansion procedure that has been adopted. In both methods, the procedure is to first evaluate a given diagram in terms of the relevant $\mathscr{T}$-matrices that appear in the diagram. Presumably, if the exact form was known for the T- and K-matrices, each diagram would then contribute a well-defined and finite amount to ϵ. However, the exact $\mathscr{T}$-matrices are not known, and the procedure is to expand each $\mathscr{T}$-matrix in powers of its arguments, to the order desired. It is apparent that at some point in this expansion procedure (which will vary from diagram to diagram) the powers of the momentum arguments of the $\mathscr{T}$-matrices in the integral corresponding to the contribution to ϵ from the given diagram, will sufficiently outweigh the powers of the momentum variables in the energy denominators to lead to divergent results. It is also apparent that from the set of diagrams containing a given number of $\mathscr{T}$-matrices, the divergence will show up earliest (i.e., in lowest order in the series for ϵ) in those diagrams of the set which contain the maximum number of particle lines. This occurs because the divergences come from high ($\gg k_F$) momenta values, and each hole line in a diagram, being restricted to momenta less than k_F, cannot contribute to the divergence.

With this in mind, we now examine the class of Goldstone diagrams containing four K-matrix interactions, and three hole lines (one I hole line and two B hole lines). (We indicate later how the same results can be achieved by the use of the F method.) The basic diagrams of this class are shown in Fig. 13. Each of these diagrams is to be completed by the addition of the two unshown B hole lines, which in each case can be performed in two ways, leading to a total of 24 Goldstone diagrams. The leading order contribution of each diagram is found by replacing each K-matrix by the constant factor $4\pi a$. Just as in [A], it is now easy to see that each diagram is logarithmically divergent. It is apparent that the leading divergence

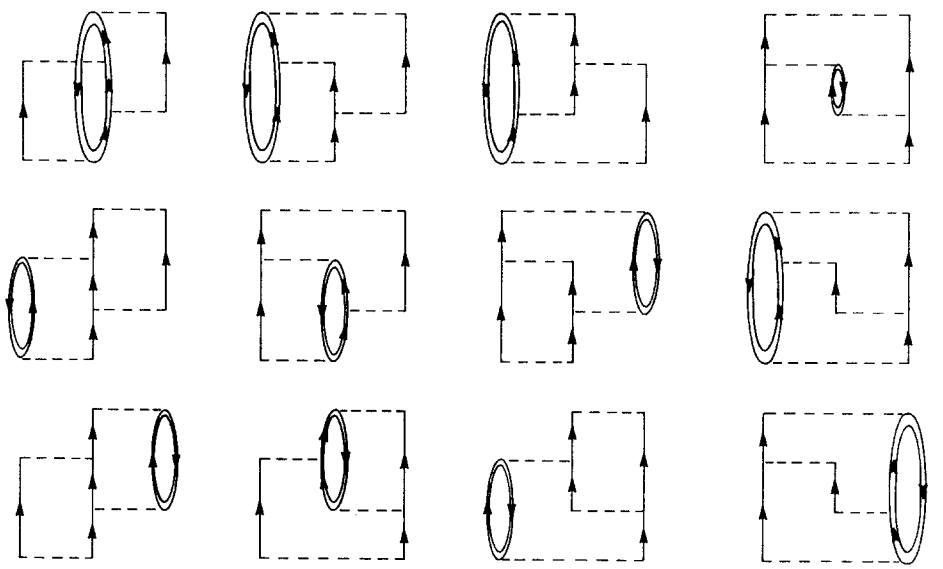

FIG. 13. The basic Goldstone diagrams containing four K-matrix interactions, and one I hole line and two B hole lines (unshown).

can be exactly isolated by replacing each hole momentum in the energy denominators by zero, and in this case all of the diagrams give an equal contribution to ϵ, apart from the trivial difference of spin–isopin factors, in the case when $m_B = m_I$. The details of this procedure for isolating the leading divergence are discussed fully in [*A*], and are not repeated here. (The unequal mass case is treated in exactly the same way, but since the diagrams have to be treated separately and the integrals cannot be evaluated exactly, which only obscures the relevant details, we do not discuss this case further.) Denoting the leading order contribution to ϵ from all 24 diagrams by ϵ_6, it is easily found that

$$\epsilon_6 = -12\nu(\nu - 1)(4\pi a/m)^4 (1/(2\pi)^{12})(4\pi k_F{}^3/3)^2 (2m)^3 \times \int_{>k_F} d\mathbf{p}\, d\mathbf{q}\, (1/2p^2)[1/(p^2 + q^2 + |\mathbf{p} + \mathbf{q}|^2)](1/2q^2),$$

which is readily simplified to the expression

$$\epsilon_6 = -(k_F{}^2/m)\, \nu(\nu - 1)(4/3\pi^6) J c^4, \tag{5.1}$$

where J is the divergent integral written in dimensionless form as

$$J = \int_1^\infty \frac{d\mathbf{p}}{p^2} \int_1^\infty \frac{d\mathbf{q}}{q^2(p^2 + \mathbf{p}\cdot\mathbf{q} + q^2)}.$$

It is trivial to reduce J to the following form, which exactly isolates its divergent piece as,

$$J = \frac{8\pi^4}{3} \int_1^\infty \frac{dp}{p}. \tag{5.2}$$

From our previous discussion we realize that the divergence is due to the expansion of the K-matrix inside the integral, and if the exact expression was known, there would presumably be a natural cutoff at $pk_F \sim a^{-1}$. Thus in the integral (5.2) the upper limit is replaced by c^{-1}, which is exact to $O(c^4 \ln c)$. The final result is thus,

$$\epsilon_6 = (k_F{}^2/m)\, \nu(\nu - 1)(32/9\pi^2)\, c^4 \ln c; \qquad m_B = m_I \equiv m. \tag{5.3}$$

From the derivation, it is apparent that no other fourth-order Goldstone diagrams will contribute to this order, since they all contain at least one more hole line (and correspondingly, at least one less particle line). Thus, the only other possible contributors to this order are the diagrams of Section 4. It is clear that the first-order diagram cannot contribute, since it contains no particle lines; and there are no valid second-order (Goldstone) diagrams. Thus, we need only consider the third-order diagrams, and in particular we select the subset of third-order diagrams containing the largest number of particle lines, namely three. These comprise the diagrams of Figs. 11 and 12, plus the set (called P_3 in Section 4) of diagrams obtained from Fig. 10 by reversing the direction of the arrows shown; twelve diagrams in all. The leading singularity is again isolated as above, by equating to zero all hole momenta in the energy denominators of the twelve diagrams, and in the arguments of the scattering functions. Again we consider only the equal mass case ($m_I = m_B \equiv m$) for ease, and it is not difficult to show that the above prescription leads to a contribution to ϵ from these twelve diagrams, say $\tilde{\epsilon}$, given by

$$\tilde{\epsilon} = 3\nu(\nu - 1)\, \frac{1}{m^3}\, \frac{1}{(2\pi)^9} \left(\frac{4\pi k_F{}^3}{3}\right)^2 (2m)^2 \int d\mathbf{p}\, (1 - n_p)$$

$$\times\, k(0, 0; \mathbf{p}, -\mathbf{p})\, \frac{1}{2p^2} \{k(\mathbf{p}, 0; \mathbf{p}, 0) + k(\mathbf{p}, 0; 0, \mathbf{p})\}\, \frac{1}{2p^2}\, k(\mathbf{p}, -\mathbf{p}; 0, 0). \tag{5.4}$$

The expression (5.4) will contain a contribution to ϵ of $O(c^4 \ln c)$, say ϵ_7, if the product of k-matrices contains a term proportional to p^2. If each of the k-matrices are written in the c.m. representation as $k(\mathbf{p}, \mathbf{p}'; s)$, the first and third k-matrices in Eq. (5.4) have $s(\equiv\kappa^2) > 0$, and in this case it was shown in [*A*] that $k(\mathbf{p}, \mathbf{p}'; s)$ is an even function of its arguments. Thus in Eq. (5.4) the first and third k-matrices may be replaced by $4\pi a$. However, if the term in Eq. (5.4) in braces, say $E(p)$, is written in the c.m. representation,

$$E(p) = \{k(\tfrac{1}{2}\mathbf{p}, \tfrac{1}{2}\mathbf{p}; -\tfrac{3}{4}p^2) + k(\tfrac{1}{2}\mathbf{p}, -\tfrac{1}{2}\mathbf{p}; -\tfrac{3}{4}p^2)\}, \tag{5.5}$$

we see that both k-matrices have $s = -\frac{3}{4}p^2$, or $\kappa = \pm(i\sqrt{3}/2)p$. The k-matrix is only defined for κ real, and when κ becomes imaginary, it becomes necessary to analytically continue the function into the complex κ-plane. It is apparent from their definitions that the functions $t(s)$ and $t^{\dagger}(s)$ provide the correct analytic continuations of $k(s)$ into the upper and lower half planes respectively. It is well-known [9] that the hard-core t-matrix has the expansion

$$t(\mathbf{p}, \mathbf{p}'; s) = 4\pi a(1 - i\kappa a) + O(a^3),$$

and choosing $\kappa = +i(\sqrt{3}/2)p$ in Eq. (5.5) leads to

$$E(p) = 2(4\pi a)(1 + (\sqrt{3}/2)pa) + O(p^2).$$

Thus, keeping the term linear in p gives the divergent term of Eq. (5.3) correctly as

$$\epsilon_7 = \left(\frac{k_F^2}{m}\right) \nu(\nu - 1) \frac{8\sqrt{3}}{3\pi^3} c^4 \int_{k_F}^{\infty} \frac{dp}{p}.$$

Replacing the upper limit of this integral by a^{-1} as before, leads to

$$\epsilon_7 = -(k_F^2/m)\, \nu(\nu - 1)(8\sqrt{3}/3\pi^3)\, c^4 \ln c; \qquad m_B = m_I \equiv m. \tag{5.6}$$

From the previous discussion it is clear that the contributions ϵ_6 and ϵ_7 exhaust the term in the series for ϵ proportional to $c^4 \ln c$. Their sum gives the total contribution,

$$\epsilon_{\log} = (k_F^2/m)\, \nu(\nu - 1)(8/9\pi^3)(4\pi - 3\sqrt{3})\, c^4 \ln c; \qquad m_B = m_I \equiv m. \tag{5.7}$$

From our comparison of the two methods (F and G) in Sections 3 and 4, it should be clear how the result of Eq. (5.7) is obtained by use of the F method.

6. Summary

In Sections 3–5 the first four terms in a series for ϵ, the ground-state energy per impurity particle, were developed for a system comprising a large number of identical background particles (B) and a relatively few number of distinct impurity particles (I). Purely for ease, the BB and BI hard-core potential interaction diameters were chosen equal (to a), and the impurities were considered to be dilute enough for II interactions to be ignored. The expansion parameter of the series is $c \equiv k_F a$, where k_F is the Fermi wavenumber of the background particles. Two distinct methods were presented, for the calculation; one employing the modified time-dependent perturbation theory of Goldstone (G method), the other using the time-independent (Feynman diagrams) Green function formulation (F method).

The various contributions (ϵ_1 through ϵ_7) to ϵ, developed in Sections 3–5, are collected together and presented below for several different situations.

Case (a): equal mass ($m_I = m_B \equiv m$).

If the background and impurity particles have the same mass m, then ϵ can be evaluated exactly to $O(c^4 \ln c)$;

$$\epsilon = \left(\frac{k_F^2}{m}\right) \nu \left[\frac{2}{3}\left(\frac{c}{\pi}\right) + \left(\frac{c}{\pi}\right)^2 + \left\{\left(\frac{4}{3} + \frac{2\pi^2}{45}\right) + (\nu - 1)\frac{8}{3}\left(\frac{\pi^2}{8} + \frac{2}{15}\ln 2 - \frac{7}{30}\right)\right\}\left(\frac{c}{\pi}\right)^3 + (\nu - 1)\frac{8}{9\pi^3}(4\pi - 3\sqrt{3})\, c^4 \ln c + O(c^4)\right],$$

where each background particle has ν spin–isospin degrees of freedom.

Case (b): equal mass; no BB interaction.

If the background particles do not interact among themselves, many of the diagrams in the series for ϵ are zero. Thus the diagrams leading to the contributions ϵ_1 to ϵ_4 contain only *BI* interactions, but those giving ϵ_5 contain a *BB* interaction and hence do not contribute in this case. Similarly, only the first diagram of Fig. 13 contributes to ϵ_6, and only the two diagrams of Figs. 10(a) and 11 contribute to ϵ_7, when the *BB* interaction vanishes. It is easily seen that in this case ϵ is given by the expression[2]

$$\epsilon = \left(\frac{k_F^2}{m}\right) \nu \left[\frac{2}{3}\left(\frac{c}{\pi}\right) + \left(\frac{c}{\pi}\right)^2 + \left(\frac{4}{3} + \frac{2\pi^2}{45}\right)\left(\frac{c}{\pi}\right)^3 + (\nu - 1)\frac{4}{27\pi^3}(2\pi - 3\sqrt{3})\, c^4 \ln c + O(c^4)\right].$$

Case (c): Λ-particle in nuclear matter.

When $m_B \neq m_I$, ϵ has to be evaluated numerically (except for the first two terms in the series). The integrations have been performed for the parameters relevant to the infinite hypernucleus; $m_B \equiv m_N(939\text{ MeV})$, $m_I \equiv m_\Lambda(1115\text{ MeV})$,

[2] This case can also be used to describe the situation of mutually interacting *B* particles, if the *BB* interaction is represented by the effective mass approximation ($m_B \to m_B^*$), and if the effective mass m_B^* of the background particles is equal to m_I. Similarly if $m_B^* \neq m_I$, one can numerically evaluate the contributions from the diagrams containing no *BB* interactions.

$\nu = 4$. The result in this case for the ground-state energy of the Λ-particle is

$$\epsilon_\Lambda = \left(\frac{k_F^2}{2\mu}\right)[0.849c + 0.393c^2 + 1.41c^3 + O(c^4 \ln c)],$$

$$\mu = m_\Lambda m_N/(m_\Lambda + m_N).$$

Using the F method, Eq. (3.1) can also be solved for nonzero momentum $\mathbf{p}$ of the impurity to give a solution for the excitation spectrum, $p_0 = \epsilon(p) + i\gamma(p)$. If $\epsilon(p)$ is written in the form

$$\epsilon(p) = (p^2/2m_I) + F(p),$$

one can make a Taylor expansion of $F(p)$ at $p = 0$ to obtain

$$\epsilon(p) - \epsilon \equiv p^2/2m_I^* = (p^2/2m_I) + (p^2/2)\,F''(0),$$

since $F'(0) = 0$, and where this equation defines the effective mass m_I^* of the impurity. In a previous paper [6] the ratio m_I^*/m_I was evaluated to $O(c^2)$ and found to be given by the expression,

$$\frac{m_I}{m_I^*} = 1 - \frac{2\nu}{3\pi^2}\left[\frac{1}{\alpha} - \frac{(1-\alpha)^2}{2\alpha^2}\ln\left(\frac{1+\alpha}{1-\alpha}\right)\right]c^2 + O(c^3),$$

$$\alpha = (m_I - m_B)/(m_I + m_B).$$

It is interesting to note that there is no term of first order in c in this expression, since the term proportional to a in the expansion of the proper self-energy $\Sigma(\mathbf{p}, p_0)$ is a constant. From our derivation of the leading logarithmic term in the series for ϵ, it is clear that there will similarly be no term in the expansion for m_I^*/m_I proportional to $c^4 \ln c$. It is not difficult to see that the leading singular term will be proportional to $c^5 \ln c$, although the calculation of its numerical coefficient is formidable.

We note that the F method must be used to calculate the damping (or imaginary) term $\gamma(p)$ of the impurity quasiparticle spectrum, and for completeness the leading order expression found in [6] for the equal mass case ($m_B = m_I \equiv m$) is given below.

$$\gamma(p) = -\frac{\nu}{15\pi}\left(\frac{k_F^2}{m}\right)c^2 \times \begin{cases} 2y^4; & 0 < y < 1 \\ (5y - 3/y); & y > 1, \end{cases}$$

$$y \equiv p/k_F\,.$$

It is clear from the calculations of Sections 3 and 4 that both the F and G methods provide powerful tools for the computation of ϵ. The two methods are in many

senses complementary, and can be used together to great advantage. The chief drawback of the F method is the large amount of bookkeeping that has to be done to keep track of the many cancellations that occur because of the quite complex form of the T-matrix Feynman diagrams. By contrast, the cancellations are taken care of very automatically and economically in the G method. On the other hand, the F method combines into a small set of diagrams, what in the G method in high order calculations can be a considerably larger class of diagrams. In addition to this, the F method also provides an easier formalism for the actual evaluation of such sets of diagrams, in many cases. In final summary we see that where the one method is weak, the other often proves strong, and a judicious combination of the two methods would appear to offer considerable advantages.

Appendix

In this appendix, the exact analytic expressions are derived for the integrals that occur in the expressions for the $O(a^3)$ terms of ϵ_3, ϵ_4, and ϵ_5, in the case of equal mass ($\alpha = 0$) for the impurity and background particles.

The integrals needed for the evaluation of ϵ_3 and ϵ_4 are given in Eqs. (3.7) and (3.12) respectively as

$$K \equiv \int_0^1 dx\, f^2(x); \qquad L \equiv \int_1^\infty dx\, f^2(x) \tag{A.1}$$
$$f(x) = \tfrac{1}{2}(1 - x^2) \ln |(1 + x)/(1 - x)| + x.$$

Using the fact that $f(x) = -f(-x)$, which follows from its definition, K may be written as

$$K = \tfrac{1}{2} \int_{-1}^1 dx\, f^2(x). \tag{A.2}$$

Making the substitution $x = -i \tan \pi z'$ in Eq. (A.2) leads to the expression,

$$K = \frac{i\pi}{2} \int_{-i\infty}^{i\infty} \frac{dz'}{\cos^6 \pi z'} [\pi z' + \sin \pi z' \cos \pi z']^2.$$

It is convenient to make the further substitution $z' = z - \frac{1}{2}$, which yields

$$K = \frac{i\pi}{2} \int_{\frac{1}{2}-i\infty}^{\frac{1}{2}+i\infty} \frac{dz}{\sin^6 \pi z} [\pi(z - \tfrac{1}{2}) - \tfrac{1}{2} \sin 2\pi z]^2. \tag{A.3}$$

At this point the integral can be converted into a very convenient contour integral,

by making use of a trick of Onsager *et al.* [11]. If the integrand of Eq. (A.3) is written as

$$F(z) = \operatorname{cosec}^6 \pi z[\pi^2(z - \tfrac{1}{2})^2 - \pi(z - \tfrac{1}{2}) \sin 2\pi z + \tfrac{1}{4}\sin^2 2\pi z], \qquad (A.4)$$

it is easy to write $F(z)$ in the form

$$F(z) = g(z) - g(z - 1)$$

by making use of the trivial algebraic identities

$$1 = z - (z - 1),$$

$$z - \tfrac{1}{2} = \tfrac{1}{2}z^2 - \tfrac{1}{2}(z - 1)^2,$$

$$(z - \tfrac{1}{2})^2 = \tfrac{1}{12}\{4z^3 - z\} - \tfrac{1}{12}\{4(z - 1)^3 - (z - 1)\}.$$

Since the trigonometric expressions in (A.4) are invariant under the change $z \to z - 1$, Eq. (A.3) can be written as

$$K = \frac{i\pi}{2} \int_{\frac{1}{2}-i\infty}^{\frac{1}{2}+i\infty} dz\, [g(z) - g(z - 1)], \qquad (A.5)$$

where

$$g(z) = \frac{z}{\sin^6 \pi z}\left[\pi^2\left(\frac{1}{3}z^2 - \frac{1}{12}\right) - \frac{\pi}{2} z \sin 2\pi z + \frac{1}{4}\sin^2 2\pi z\right]. \qquad (A.6)$$

The second term in Eq. (A.5) is rewritten by letting $z - 1 = z'$, to give

$$K = \frac{i\pi}{2} \oint_C dz\, g(z), \qquad (A.7)$$

where the contour C, which completely surrounds the imaginary axis, contains only one (fifth-order) pole at $z = 0$. From Eq. (A.6), the residue at $z = 0$ is readily evaluated, and the result

$$K = (2\pi^2/45) + \tfrac{1}{3}, \qquad (A.8)$$

is easily obtained.

The substitution $x^{-1} = -i \tan \pi z$ in Eq. (A.1) leads to the expression for L,

$$L = -\frac{i\pi}{2} \int_{\sigma-i\infty}^{\sigma+i\infty} \frac{dz}{\sin^6 \pi z}\, [\pi z - \tfrac{1}{2} \sin 2\pi z]^2; \qquad |\sigma| < 1$$

where σ is real. Choosing $0 < \sigma < 1$, allows the same contour C as above to be used, and similar techniques lead to the result,

$$L = (4\pi^2/45) - \tfrac{1}{3}. \tag{A.9}$$

In the equal mass case ($m_B = m_I \equiv m$), the integral needed for the evaluation of ϵ_5 in Eq. (3.14) is

$$M = i \int \frac{d^4q}{(2\pi)^4} \frac{\Pi^2(q)}{q_0 - q^2 + i\eta}, \tag{A.10}$$

where

$$\Pi(q) = -i \int \frac{d^4t}{(2\pi)^4} G_B{}^0(t)\, G_B{}^0(t+q), \tag{A.11}$$

and where for convenience we employ units $2m = k_F = 1$. The t_0-integration in Eq. (A.11) is readily performed to give

$$\begin{aligned} \Pi(\mathbf{q}, q_0) &\equiv \Pi(q) \\ &= 2 \int \frac{d\mathbf{t}}{(2\pi)^3} n_t(1 - n_{t+q}) \frac{\omega_{qt}}{(q_0 - \omega_{qt} + i\eta)(q_0 + \omega_{qt} - i\eta)}, \\ \omega_{qt} &\equiv |\,\mathbf{q} + \mathbf{t}\,|^2 - t^2, \\ n_t &\equiv n(t) = \theta(1 - |\,\mathbf{t}\,|). \end{aligned} \tag{A.12}$$

Substituting for $\Pi(q)$ from Eq. (A.12) into Eq. (A.10) yields, after the q_0-integration has been performed,

$$M = -2 \int \frac{d\mathbf{q}\, d\mathbf{s}}{(2\pi)^6} \frac{n_s(1 - n_{s+q})}{q^2 + \omega_{qs}} \operatorname{Re} \Pi(\mathbf{q}, \omega_{qs}). \tag{A.13}$$

Equation (A.12) immediately yields the real part of $\Pi(q)$ as

$$\operatorname{Re} \Pi(\mathbf{q}, q_0) = 2 \int \frac{d\mathbf{t}}{(2\pi)^3} n_t(1 - n_{t+q}) \frac{\omega_{qt}}{q_0{}^2 - (\omega_{qt})^2}.$$

The second term of this equation vanishes identically since the product of step functions is even under the interchange $\mathbf{t} \leftrightarrows \mathbf{t} + \mathbf{q}$,while ω_{qt} is odd. The remaining term is readily evaluated to give

$$\operatorname{Re} \Pi(\mathbf{q}, q_0) = \frac{1}{8\pi^2 q} \left\{ f\left(\frac{q_0 - q^2}{2q}\right) - f\left(\frac{q_0 + q^2}{2q}\right) \right\}, \tag{A.14}$$

where $f(x)$ is defined in Eq. (A.1). After substituting from Eq. (A.14), and putting $\mathbf{s} = -\mathbf{q} - \mathbf{t}$, Eq. (A.13) becomes

$$M = 2 \int \frac{d\mathbf{q}\, d\mathbf{t}}{(2\pi)^6} \frac{n_{\mathbf{q}+\mathbf{t}}(1 - n_t)}{2\mathbf{q} \cdot \mathbf{t}} \frac{1}{8\pi^2 q} \{f(-q - \hat{q} \cdot \mathbf{t}) - f(-\hat{q} \cdot \mathbf{t})\},$$

and using that $f(x)$ is an odd function, hence

$$M = \frac{1}{(2\pi)^6} \int t\, dt \int \frac{du}{u} \int dq\, (1 - n_t)\, n_{\mathbf{q}+\mathbf{t}} \{f(tu) - f(q + tu)\},$$

where $u \equiv \hat{q} \cdot \hat{t}$, and the other angular integrations have been performed. It is now easy to convert the product of step functions into limits of integration, as a result of which we find,

$$M = (I_1 + I_2)/(2\pi)^6, \tag{A.15}$$

where

$$\begin{aligned} I_1 &= \int_1^\infty t\, dt \int_{(t^2-1)^{1/2}}^t \frac{dx}{x} \int_{x-(1-t^2+x^2)^{1/2}}^{x+(1-t^2+x^2)^{1/2}} dq\, f(x), \\ I_2 &= \int_1^\infty t\, dt \int_{(t^2-1)^{1/2}}^t \frac{dx}{x} \int_{x-(1-t^2+x^2)^{1/2}}^{x+(1-t^2+x^2)^{1/2}} dq\, f(q - x), \end{aligned} \tag{A.16}$$

where the substitution $u = -x/t$ has been made. By making the further substitution $q - x = z$ in Eq. (A.16) for I_2, and using that $f(z)$ is an odd function, it is apparent that

$$I_2 = 0. \tag{A.17}$$

In Eq. (A.16) for I_1, the q-integration is performed trivially, and the order of the remaining two integrations is interchanged by using

$$\int_1^\infty dt \int_{(t^2-1)^{1/2}}^t dx = \int_0^1 dx \int_1^{(x^2+1)^{1/2}} dt + \int_1^\infty dx \int_x^{(x^2+1)^{1/2}} dt.$$

The two t-integrations can then be performed, to give

$$I_1 = \tfrac{2}{3}(J_1 + J_2), \tag{A.18}$$

$$J_1 = \int_0^1 x^2 f(x)\, dx, \qquad J_2 = \int_1^\infty \frac{dx}{x} f(x).$$

Combining Eqs. (A.15–18) yields the result,

$$M = \tfrac{2}{3}(1/2\pi)^6 (J_1 + J_2). \tag{A.19}$$

The integral J_1 can be evaluated easily, and J_2 can be found by techniques similar to those used for the evaluation of K and L above, to give

$$J_1 = \tfrac{2}{15}(2 + \ln 2), \qquad J_2 = (\pi^2/8) - \tfrac{1}{2}. \tag{A.20}$$

Combining Eqs. (A.19, 20), and replacing the factors of k_F and $2m$, gives the final result

$$M = (2m)^2 k_F{}^5 \left(\frac{1}{2\pi}\right)^6 \frac{2}{3}\left(\frac{\pi^2}{8} + \frac{2}{15}\ln 2 - \frac{7}{30}\right). \tag{A.21}$$

ACKNOWLEDGMENT

It is a pleasure to thank Professor J. Dirk Walecka for many useful discussions and for his continued interest in this work.

REFERENCES

1. R. F. BISHOP, *Ann. Phys. (N.Y.)* **77** (1973), 106.
2. L. COOPER, *Phys. Rev.* **104** (1956), 1189.
3. J. D. WALECKA, *Nuovo Cimento* **16** (1960), 342.
4. A. R. BODMER AND D. M. ROTE, "Proceedings of the International Conference on Hypernuclear Physics," Vol. II, p. 521, Argonne National Laboratory, Argonne, Ill., 1969.
5. H. A. BETHE AND J. GOLDSTONE, *Proc. Roy. Soc. (London)* **A238** (1957), 551.
6. R. F. BISHOP, *Nucl. Phys.* **B17** (1970), 573.
7. H. SUGAWARA AND F. VON HIPPEL, *Phys. Rev.* **172** (1968), 1764.
8. E. E. SALPETER AND H. A. BETHE, *Phys. Rev.* **84** (1951), 1232.
9. R. F. BISHOP, *Phys. Rev. C* **7** (1973), 479.
10. J. GOLDSTONE, *Proc. Roy. Soc. (London)* **A239** (1957), 267.
11. L. ONSAGER, L. MITTAG, AND M. J. STEPHEN, *Ann. Physik* **18** (1966), 71.